Bayesian Compressive Sensing Assisted Space Time Block Coded Quadrature Spatial Modulation

Lixia Xiao, Pei Xiao, *Senior member, IEEE*, Yue Xiao, *Member, IEEE*,
Ibrahim Hemadeh, Abdelrahim Mohamed, and Lajos Hanzo, *Fellow, IEEE*

***Abstract*—A novel Multiple-Input and Multiple-Output (MIMO) transmission scheme termed as Space-Time Block Coded Quadrature Spatial Modulation (STBC-QSM) is proposed. It amalgamates the concept of Quadrature Spatial Modulation (QSM) and Space-Time Block Coding (STBC) to exploit the diversity benefits of STBC relying on sparse Radio Frequency (RF) chains. In the proposed STBC-QSM scheme, the conventional constellation points of the STBC structure are replaced by the QSM symbols, hence the information bits are conveyed both by the antenna indices as well as by conventional STBC blocks. Furthermore, an efficient Bayesian Compressive Sensing (BCS) algorithm is developed for our proposed STBC-QSM system. Both our analytical and simulation results demonstrated that the proposed scheme is capable of providing considerable performance gains over the existing schemes. Moreover, the proposed BCS detector is capable of approaching the Maximum Likelihood (ML) detector's performance despite only imposing a complexity near similar to that of the Minimum Mean Square Error (MMSE) detector in the high Signal to Noise Ratio (SNR) regions.**

***Index Terms*—Quadrature Spatial Modulation (QSM), Space Time Block Coding (STBC), Bayesian Compressive Sensing.**

I. Introduction

QUADRATURE spatial modulation (QSM) [1] is a high-efficiency MIMO technique, which exploits both the in-phase and quadrature dimensions for enhancing the overall throughput of the conventional Spatial Modulation (SM) system [2]. In the QSM scheme, both the indices of the real part as well as of the imaginary part of an M-ary amplitude phase modulation (APM) symbol and the APM symbol itself convey information, hence resulting in higher spectral efficiency than conventional SM. Furthermore, the inter-antenna interference can also be avoided by the QSM scheme, since orthogonal symbols are transmitted by the activated antennas. Therefore, QSM constitutes a promising MIMO candidate for next generation wireless communication [3]-[5].

L. Xiao, P. Xiao, I. Hemadeh and A. Mohamed are with the school of Electrical Electronic Engineering of University of Surrey.

Y. Xiao are with the National Key Laboratory of Science and Technology on Communications, University of Electronic Science and Technology of China 611731, Sichuan, China.

L. Hanzo is with the school of Electronics and Computer Science, University of Southampton, Southampton SO17 1BJ, U.K. (email: lh@ecs.soton.ac.uk).

This work was supported in part by the U.K. Engineering and Physical Sciences Research Council under Grant EP/P03456X/1 and EP/PO34284/1

The authors also would like to acknowledge the support of the University of Surrey 5GIC (http://www.surrey.ac.uk/5gic) members for this work.

L. Hanzo would like to acknowledge the financial support of the ERC's Advanced Fellow Grant QuantCom.

Recently, the QSM design efforts have been mainly focused on the performance analysis [6]-[7], on its coherent vs non-coherent detection [8]-[9], as well as on its extension to multi-carrier transmission [10]. In order to exploit the diversity gain of the QSM and SM system, the diversity oriented QSM and SM designs were investigated in [11]-[14]. Specifically, in [13], an Enhanced SM relying on an Arbitrary Transmit Antenna (ESM-ATA) configuration and single or twin RF stages was proposed. Specifically, in the ESM-ATA scheme, a novel Space Time Block Coding (STBC) based SM structure was presented, which is capable of outperforming the existing STBC-SM schemes [11] in terms of its Bit Error Ratio (BER), despite its modest complexity. However, this scheme achieves its diversity gain at the expense of a reduced transmit rate. In order to achieve a beneficial diversity gain at a high transmit rate, a Diversity-Achieving QSM (DA-QSM) scheme was proposed in [14] by amalgamating the QSM concept with the dispersion matrices. However, since the QSM scheme is a recently developed MIMO arrangement, how to exploit the diversity gain by involving the classic STBC structure has not been investigated. On the other hand, since the SM based MIMO schemes exhibit an inherent transmit symbol sparsity, Compressive Sensing (CS) has been invoked as an efficient detection tool of detecting the SM based MIMO symbols [15][16].

In order to further exploit the diversity gain of QSM system at a low-complexity, in this paper a novel STBC-QSM system relying on Efficient Bayesian CS (E-BCS) detector is investigated. Furthermore, both the diversity gain and the Average Bit Error Probability (ABEP) are analyzed for the proposed STBC-QSM system. Both the theoretical and simulation results demonstrate that the proposed STBC-QSM system is capable of providing significant performance gains over the existing QSM and STBC based SM schemes. Moreover, an Efficient Bayesian Compressive Sensing detector is proposed for our STBC-QSM system, which is capable of approaching the Maximum Likelihood (ML) detector's performance at the Minimum Mean Square Error (MMSE) detector's complexity in the high Signal to Noise Ratio (SNR) region.

II. QSM System

We consider a QSM system having N_t Transmit Antennas (TAs) and N_r Receive Antennas (RAs) operating in flat Rayleigh fading channels. In a QSM scheme, the information bits are divided into two parts, where $2\log_2(N_t)$ bits are mapped to the active TA indices and $\log_2(M)$ bits are mapped to an M-ary APM symbol x. To be specific, $\log_2(N_t)$ bits are used for selecting a specific TA for transmitting the real part of signal x and another $\log_2(N_t)$

bits are used for selecting an active TA to transmit the imaginary part of x. Based on the above mapping rule, the transmitted signal $\mathbf{x} \in \mathbb{C}^{N_t \times 1}$can be represented as

$$\mathbf{x} = \begin{cases} [\underbrace{0,...,0}_{l_{\Re}-1}, x_{\Re} + jx_{\Im}, \underbrace{0,...,0}_{N_t - l_{\Re}}]^T, \text{ if } l_{\Re} = l_{\Im} \\ [\underbrace{0,...,0}_{l_{\Re}-1}, x_{\Re}, 0, ..., 0, jx_{\Im}, \underbrace{0,...,0}_{N_t - l_{\Im}}]^T, \text{ else} \end{cases} \tag{1}$$

where $x_{\Re}$ and $x_{\Im}$ denote the real and imaginary parts of x, respectively, while $l_{\Re} = (1, ..., N_t)$ and $l_{\Im} = (1, ..., N_t)$ represent the corresponding active TA indices.

III. Proposed Space Time Block Coding Quadrature Spatial Modulation system

We propose a STBC-QSM system having N_t TAs and N_r RAs operating in the flat Rayleigh fading channels. In the proposed STBC-QSM scheme, based on the QSM mapping principle, the $2 \times [2\log_2(N_t/2) + \log_2(M)]$ information bits are first mapped to a pair of QSM symbols $\mathbf{x}_i$ $i = 1, 2$ using $N_t/2$ TAs as

$$\mathbf{x}_i = \begin{cases} [\underbrace{0,...,0}_{l^i_{\Re}-1}, x^i_{\Re} + jx^i_{\Im}, \underbrace{0,...,0}_{N_t/2 - l^i_{\Re}}]^T, & \text{if } l^i_{\Re} = l^i_{\Im} \\ [\underbrace{0,...,0}_{l^i_{\Re}-1}, x^i_{\Re}, 0, ..., 0, jx^i_{\Im}, \underbrace{0,...,0}_{N_t/2 - l^i_{\Im}}]^T, & \text{else} \end{cases} \tag{2}$$

where $l^i_{\Re}$, $l^i_{\Im}$, $x^i_{\Re}$, $x^i_{\Im}$ are the antenna indices and symbols of the QSM symbol $\mathbf{x}_i$.

Then the transmit symbol of our proposed STBC-QSM system can be expressed as

$$\mathbf{X} = \begin{bmatrix} \mathbf{x}_1 & \mathbf{x}_2 \\ -\mathbf{x}_2^* & \mathbf{x}_1^* \end{bmatrix}. \tag{3}$$

Let $\mathbf{H} \in \mathbb{C}^{N_r \times N_t}$ and $\mathbf{n} \in \mathbb{C}^{N_r \times 1}$ denote the MIMO channel matrix and the noise vector, whose elements obey the complex Gaussian distributions associated with $\mathcal{CN}(0, 1)$ and $\mathcal{CN}(0, \sigma^2)$, respectively, where σ^2 is the noise variance. According to (3), the received signal matrix $\mathbf{Y}_t \in \mathbb{C}^{N_r \times 2}$ consisting of a pair of time slots can be expressed as

$$\begin{aligned} \mathbf{Y}_1 &= [\mathbf{y}_1, \mathbf{y}_2] = \mathbf{HX} + [\mathbf{n}_1, \mathbf{n}_2] \\ &= [\mathbf{H}_1, \mathbf{H}_2] \begin{bmatrix} \mathbf{x}_1 & \mathbf{x}_2 \\ -\mathbf{x}_2^* & \mathbf{x}_1^* \end{bmatrix} + [\mathbf{n}_1, \mathbf{n}_2] \end{aligned}, \tag{4}$$

where $\mathbf{H}_1$ and $\mathbf{H}_2$ denote the first $N_t/2$ columns and second $N_t/2$ columns of $\mathbf{H}$. Hence, the optimal ML-based demodulator can be formulated as

$$\hat{\mathbf{X}} = \underset{\mathbf{X} \in \mathbb{X}_{\text{QSM}}}{\arg\min} \left\| \mathbf{Y} - \mathbf{HX} \right\|_F^2, \tag{5}$$

where $\mathbb{X}_{\text{QSM}}$ is the set of the proposed STBC-QSM symbols.

IV. Performance Analysis for the proposed STBC-QSM system

A. Diversity and Coding Gain Analysis

In this section, the diversity and coding gain of the porposed STBC-QSM system is analyzed. Assuming that the i-th and j-th STBC-QSM symbols are expressed as

$$\mathbf{X}_i = \begin{bmatrix} \mathbf{x}_1^i & \mathbf{x}_2^i \\ -(\mathbf{x}_2^i)^* & (\mathbf{x}_1^i)^* \end{bmatrix}, \mathbf{X}_j = \begin{bmatrix} \mathbf{x}_1^j & \mathbf{x}_2^j \\ -(\mathbf{x}_2^j)^* & (\mathbf{x}_1^j)^* \end{bmatrix}, \tag{6}$$

the diversity and coding gain can be expressed as [13]

$$G = \min_{\mathbf{X}_i \neq \mathbf{X}_j} |\det(\Delta^H \Delta)|, \tag{7}$$

where $\Delta = \mathbf{X}_i - \mathbf{X}_j$. According to (6), we have

$$\Delta^H \Delta = \begin{bmatrix} A_E & 0 \\ 0 & A_E \end{bmatrix}, \tag{8}$$

with $A_E = ||\mathbf{x}_1^i - \mathbf{x}_1^j||^2 + ||\mathbf{x}_2^i - \mathbf{x}_2^j||^2$, which can be further expressed as

$$A_E = \begin{cases} 0, & \text{if } \mathbf{x}_1^i = \mathbf{x}_1^j, \mathbf{x}_2^i = \mathbf{x}_2^j \\ ||\mathbf{x}_1^i - \mathbf{x}_1^j||^2, & \text{if } \mathbf{x}_1^i \neq \mathbf{x}_1^j, \mathbf{x}_2^i = \mathbf{x}_2^j \\ ||\mathbf{x}_2^i - \mathbf{x}_2^j||^2, & \text{if} \mathbf{x}_1^i = \mathbf{x}_1^j, \mathbf{x}_2^i \neq \mathbf{x}_2^j \\ ||\mathbf{x}_1^i - \mathbf{x}_1^j||^2 + ||\mathbf{x}_2^i - \mathbf{x}_2^j||^2, & \text{else.} \end{cases} \tag{9}$$

Hence, the coding gain can be expressed as

$$G_E = \min_{\mathbf{X}_i \neq \mathbf{X}_j} |\det(\Delta_E^H \Delta_E)| = \min_{\mathbf{X}_i \neq \mathbf{X}_j} (A_E^2). \tag{10}$$

According to (9), we have

$$\min_{\mathbf{X}_i \neq \mathbf{X}_j} (A_E) = \min[\min_{\mathbf{x}_1^i \neq \mathbf{x}_1^j} (||\mathbf{x}_1^i - \mathbf{x}_1^j||^2), \min_{\mathbf{x}_2^i \neq \mathbf{x}_2^j} (||\mathbf{x}_2^i - \mathbf{x}_2^j||^2)]. \tag{11}$$

Since we have

$$\min_{\mathbf{x}_1^i \neq \mathbf{x}_1^j} (||\mathbf{x}_1^i - \mathbf{x}_1^j||^2) = \min_{\mathbf{x}_2^i \neq \mathbf{x}_2^j} (||\mathbf{x}_2^i - \mathbf{x}_2^j||^2) = \delta_{\min}, \tag{12}$$

where $\delta_{\min} = \min(||\mathbf{x}_1 - \mathbf{x}_2||^2)$ denotes the minimum Euclidean Distance (ED) between any two QSM symbols $\mathbf{x}_1$ and $\mathbf{x}_2$. As a result, the coding gain can be further expressed as

$$G_E = \min_{\mathbf{x}_1 \neq \mathbf{x}_2} ({\delta_{\min}}^2). \tag{13}$$

According to (2), the ED of any two QSM symbols such as $\mathbf{x}_1$ and $\mathbf{x}_2$ can be expressed as

$$\begin{aligned} &\|\mathbf{x}_1 - \mathbf{x}_2\|^2 \\ &= \begin{cases} |x^1_{\Re} - x^2_{\Re}|^2 + |x^1_{\Im} - x^2_{\Im}|^2, & \text{if } l^1_{\Re} = l^2_{\Re}, l^1_{\Im} = l^2_{\Im}; \\ |x^1_{\Re} - x^2_{\Re}|^2 + |x^1_{\Im}|^2 + |x^2_{\Im}|^2, & \text{if } l^1_{\Re} = l^2_{\Re}, l^1_{\Im} \neq l^2_{\Im}; \\ |x^1_{\Re}|^2 + |x^2_{\Re}|^2 + |x^1_{\Im} - x^2_{\Im}|^2, & \text{if } l^1_{\Re} \neq l^2_{\Re}, l^1_{\Im} = l^2_{\Im}; \\ |x^1_{\Re}|^2 + |x^1_{\Im}|^2 + |x^2_{\Re}|^2 + |x^2_{\Im}|^2, & \text{if } l^1_{\Re} \neq l^2_{\Re}, \Im^1 \neq l^2_{\Im}. \end{cases} \end{aligned} \tag{14}$$

Then the value of $\delta_{\min}$ can be further expressed as

$$\begin{aligned} \delta_{\min} &= \min_{\mathbf{x}_1 \neq \mathbf{x}_2} (\|\mathbf{x}_1 - \mathbf{x}_2\|^2) \\ &= \min_{\mathbf{x}_1 \neq \mathbf{x}_2} [\min_{x^1_{\Im} = x^2_{\Im}} (|x^1_{\Re}|^2 + |x^2_{\Re}|^2), \min_{x^1_{\Re} = x^2_{\Re}} (|x^1_{\Im}|^2 + |x^2_{\Im}|^2)]. \end{aligned} \tag{15}$$

Finally, the code gain of the proposed STBC-QSM scheme is expressed as

$$G_E = \min_{\mathbf{x}_1 \neq \mathbf{x}_2} [\min_{x^1_{\Im} = x^2_{\Im}} (|x^1_{\Re}|^2 + |x^2_{\Re}|^2)^2, \min_{x^1_{\Re} = x^2_{\Re}} (|x^1_{\Im}|^2 + |x^2_{\Im}|^2)^2]. \tag{16}$$

In order to provide further insights, the maximum coding gain comparisons between the proposed STBC-QSM scheme and the existing scheme are presented in Table I. Observe from Table I that the coding gain of the proposed STBC-QSM scheme is only dependent on the constellation size and it is higher than that of the existing ESM-ATA system.

TABLE I
MAXIMUM CODING GAIN COMPARISONS BETWEEN THE PROPOSED STBC-QSM SCHEME AND EXISTING SCHEMES.

$N_t = 4$		
	Rate=4 bits	Rate=6 bits
ESM-ATA [7]	0.4442	0.0400
Proposed STBC-QSM	1	0.04
$N_t = 8$		
	Rate=6 bits	Rate=8 bits
ESM-ATA [7]	0.16	0.0091
Proposed STBC-QSM	1	0.04

B. ABEP Analysis of STBC-QSM

Let us now denote the transmit and receive signal of STBC-QSM by $\mathbf{X}_i$ and $\mathbf{X}_j$, respectively. Then the ABEP upper bound is given by

$$P_b = \frac{1}{2B2^{2B}} \sum_{i=1}^{2^{2B}} \sum_{j=1, j\neq i}^{2^{2B}} d(\mathbf{X}_i, \mathbf{X}_j) P(\mathbf{X}_i \to \mathbf{X}_j), \quad (17)$$

where $d(\mathbf{X}_i, \mathbf{X}_j)$ is the number of error bits and $P(\mathbf{X}_i \to \mathbf{X}_j)$ denotes the Pairwise Error Probability (PEP). According to [13], the value of $P(\mathbf{X}_i \to \mathbf{X}_j)$ can be obtained by Eq. (18), where $\kappa_{i,j}$ is the rank of the distance matrix $\mathbf{D}_{i,j} = (\mathbf{X}_i - \mathbf{X}_j)(\mathbf{X}_i - \mathbf{X}_j)^H$, and $\lambda_{i,j,1}, \cdots, \lambda_{i,j,\kappa_{i,j}}$ are the non-zero eigenvalues of $\mathbf{D}_{i,j}$.

V. BAYESIAN COMPRESSIVE SENSING DETECTION FOR OUR STBC-QSM SYSTEM

A. Bayesian CS Detection

In order to reduce the complexity of the ML detector, in this section Bayesian CS (BCS) aided detection is investigated in the context of our proposed STBC-QSM system. Firstly, Eq. (4) can be represented as

$$\underbrace{\begin{bmatrix} \mathbf{y}_1 \\ \mathbf{y}_2^* \end{bmatrix}}_{\mathbf{y}} = \underbrace{\begin{pmatrix} \mathbf{H}_1 & -\mathbf{H}_2 \\ \mathbf{H}_2^* & \mathbf{H}_1^* \end{pmatrix}}_{\mathbf{W}} \underbrace{\begin{pmatrix} \mathbf{x}_1 \\ \mathbf{x}_2^* \end{pmatrix}}_{\mathbf{x}} + \underbrace{\begin{pmatrix} \mathbf{n}_1 \\ \mathbf{n}_2^* \end{pmatrix}}_{\mathbf{n}}. \quad (19)$$

Observe from (19) that the sparsity of $\mathbf{x}$ is varied from $2, 3, 4$. In order to make the sparsity of the transmit symbol a constant, (19) is formulated in the real valued field as

$$\underbrace{\begin{bmatrix} \Re(\mathbf{y}) \\ \Im(\mathbf{y}) \end{bmatrix}}_{\tilde{\mathbf{y}}} = \underbrace{\begin{bmatrix} \Re(\mathbf{W}) & -\Im(\mathbf{W}) \\ \Im(\mathbf{W}) & \Re(\mathbf{W}) \end{bmatrix}}_{\tilde{\mathbf{W}}} \underbrace{\begin{bmatrix} \Re(\mathbf{x}) \\ \Im(\mathbf{x}) \end{bmatrix}}_{\tilde{\mathbf{x}}} + \underbrace{\begin{bmatrix} \Re(\mathbf{n}) \\ \Im(\mathbf{n}) \end{bmatrix}}_{\tilde{\mathbf{n}}}, \quad (20)$$

where $\tilde{\mathbf{y}} \in \Re^{4N_r \times 1}$, $\tilde{\mathbf{W}} \in \Re^{4N_r \times 2N_t}$, $\tilde{\mathbf{x}} \in \Re^{2N_t \times 1}$ and $\tilde{\mathbf{n}} \in \Re^{4N_r \times 1}$. Therefore, the sparsity of $\tilde{\mathbf{x}}$ becomes four, and the indices of the nonzero elements are distributed as $l^1_{\Re}, l^2_{\Re} + N_t/2, l^1_{\Im} + N_t, l^1_{\Im} + 3N_t/2$, which can be beneficially exploited for BCS detection. In the context of BCS detection [8], the transmit symbol is estimated as

$$\hat{\mathbf{x}} = \arg\max_{\tilde{\mathbf{x}}} p(\tilde{\mathbf{y}}|\tilde{\mathbf{x}}), \quad (21)$$

where we have

$$p(\tilde{\mathbf{y}}|\tilde{\mathbf{x}}) = (2\pi\sigma^2)^{-2N_r} \exp(-\frac{\left\|\tilde{\mathbf{y}} - \tilde{\mathbf{W}}\tilde{\mathbf{x}}\right\|^2}{2\sigma^2}). \quad (22)$$

According to (20), the density of $\tilde{\mathbf{x}}$ conditioned on γ is Gaussian, formulated as

$$p(\tilde{\mathbf{x}}; \gamma) = \prod_{i=1}^{2N_t} \sqrt{2\pi\gamma_i} \exp(-\frac{\tilde{x}_i^2}{2\gamma_i}), \quad (23)$$

where $\gamma = [\gamma_1, ..., \gamma_{2N_t}]$ denotes the variance vector of $\tilde{\mathbf{x}}$. Then Eq. (21) can be reformulated as

$$(\hat{\mathbf{x}}, \hat{\gamma}) = \arg\max_{(\tilde{\mathbf{x}}, \gamma)} p([\tilde{\mathbf{x}}, \gamma]|\tilde{\mathbf{y}}), \quad (24)$$

where we have

$$p([\tilde{\mathbf{x}}, \gamma]|\tilde{\mathbf{y}}) = p(\tilde{\mathbf{x}}|\tilde{\mathbf{y}}; \gamma) p(\gamma|\tilde{\mathbf{y}}). \quad (25)$$

The value of $p(\tilde{\mathbf{x}}|\tilde{\mathbf{y}}; \gamma)$ obeys the Gaussian distribution formulated as

$$p(\tilde{\mathbf{x}}|\tilde{\mathbf{y}}; \gamma) \sim N(\mu, \Sigma), \quad (26)$$

with the mean and variance vector given by

$$\begin{aligned} \mu &= \mathbf{\Gamma}\tilde{\mathbf{W}}^T {\Sigma_{\tilde{\mathbf{y}}}}^{-1} \tilde{\mathbf{y}} \\ \Sigma &= \mathbf{\Gamma} - \mathbf{\Gamma}\tilde{\mathbf{W}}^T {\Sigma_{\tilde{\mathbf{y}}}}^{-1} \tilde{\mathbf{W}}\mathbf{\Gamma} \end{aligned}, \quad (27)$$

where we have $\Sigma_{\tilde{\mathbf{y}}} = \sigma^2 I + \tilde{\mathbf{W}}\mathbf{\Gamma}\tilde{\mathbf{W}}^T$ and $\mathbf{\Gamma} = diag(\gamma)$. According to [8], the variance vector can be updated as

$$\gamma_i^{\text{new}} = \frac{|\mu_i|^2}{4N_r(1 - \gamma_i^{-1}\Sigma_{i,i})}, i = 1, ..., 2N_t, \quad (28)$$

where μ_i and $\Sigma_{i,i}$ denote the i-th element of μ and the i-th diag element of Σ, respectively. Since the activated indices of (20) are special, the elements of $\{\gamma_i^{\text{new}}\}_{i=1}^{2N_t}$ can be divided into four parts and sorted in descending order as

$$\begin{aligned} &\hat{\gamma}_1 = [\hat{\gamma}_1^1, ..., \hat{\gamma}_1^{\frac{N_t}{2}}], \hat{\gamma}_1^1 > \cdots > \hat{\gamma}_1^{\frac{N_t}{2}} \in (1, \tfrac{N_t}{2}); \\ &\hat{\gamma}_2 = [\hat{\gamma}_2^1, ..., \hat{\gamma}_2^{\frac{N_t}{2}}], \hat{\gamma}_2^1 > \cdots > \hat{\gamma}_2^{N_t/2} \in (\tfrac{N_t}{2} + 1, N_t); \\ &\hat{\gamma}_3 = [\hat{\gamma}_3^1, ..., \hat{\gamma}_3^{\frac{N_t}{2}}], \hat{\gamma}_3^1 > \cdots > \hat{\gamma}_3^{N_t/2} \in (N_t + 1, \tfrac{3N_t}{2}); \\ &\hat{\gamma}_4 = [\hat{\gamma}_4^1, ..., \hat{\gamma}_4^{\frac{N_t}{2}}], \hat{\gamma}_4^1 > \cdots > \hat{\gamma}_4^{N_t/2} \in (\tfrac{3N_t}{2} + 1, 2N_t). \end{aligned} \quad (29)$$

Finally, the activated indices of (20) can be obtained as $\Lambda = (l^1_{\Re}, l^2_{\Re}, l^1_{\Im}, l^2_{\Im}) = (\hat{\gamma}_1^1, \hat{\gamma}_2^1, \hat{\gamma}_3^1, \hat{\gamma}_4^1)$ and the corresponding constellation symbols are estimated as

$$(x^1_{\Re}, x^2_{\Re}, x^1_{\Im}, x^2_{\Im}) = \mathbb{Q}[((\tilde{\mathbf{W}}_\Lambda)^H \tilde{\mathbf{W}}_\Lambda + \sigma^2 \mathbf{I}_4)^{-1} (\tilde{\mathbf{W}}_\Lambda)^H \tilde{\mathbf{y}}], \quad (30)$$

where $\mathbb{Q}(\cdot)$ denotes the digital demodulation function and $\tilde{\mathbf{W}}_\Lambda$ represents the sub-matrix of $\tilde{\mathbf{W}}$ including Λ columns.

B. Efficient Bayesian CS Detection

In order to further improve the performance of the BCS detector, an efficient BCS detector is proposed for our STBC-QSM system. In the proposed E-BCS detector, specific thresholds are employed for eliminating the inaccurate results estimated by the BCS detector. As for the inaccurate results, we increase the search space to improve the attainable performance gain. The E-BCS detector operates as follows.

Step 1: Obtain $\hat{\gamma}_1$, $\hat{\gamma}_2$, $\hat{\gamma}_3$ and $\hat{\gamma}_4$ by (29).

Step 2: Determine wether the estimated indices are right or not; If we have $\hat{\gamma}_j^1 < V_{\text{th}}^1$ or $(\hat{\gamma}_j^1/\hat{\gamma}_j^2) < V_{\text{th}}^2$, $j = (1, ..., 4)$, the estimated indices $\hat{\gamma}_j^1$ are regarded as being inaccurate; Otherwise, as accurate.

Step 3: For the inaccurate indices $\hat{\gamma}_j^1$, we choose m elements from $\hat{\gamma}_j$ as candidates, so that we can glean N_m possible estimated indices hosted by the set $(\Lambda_1, ..., \Lambda_{N_m})$.

Step 4: For each index set Λ_q $q = (1, ..., N_m)$ of Step 3, the corresponding symbol vector $\mathbf{s}_q$ can be estimated by (30).

Algorithm 1 The proposed E-BCS detector

Input: $\tilde{\mathbf{y}}$, $\tilde{\mathbf{W}}$;
Output: $\Lambda = (l^1_{\Re}, l^2_{\Re}, l^1_{\Im}, l^2_{\Im}), \hat{\mathbf{s}} = (x^1_{\Re}, x^2_{\Re}, x^1_{\Im}, x^2_{\Im})$;
1: Compute the mean value μ and covariance matrix Σ using (27).
2: Compute the variance vector γ_i^{new} using (28).
3: Obtain the sorted 4 group values of γ_i^{new} of (29) as $\hat{\gamma}_1$, $\hat{\gamma}_2$, $\hat{\gamma}_3$ and $\hat{\gamma}_4$.
4: **for** $j \in (1, 4)$ **do**
5: **if** $\hat{\gamma}_j^1 < V_{\text{th}}^1$ or $(\hat{\gamma}_j^1/\hat{\gamma}_j^2) < V_{\text{th}}^2$ **then**
6: $L_j = \hat{\gamma}_j^1$;
7: **else**
8: $L_j = [\hat{\gamma}_j^1, ..., \hat{\gamma}_j^m]$;
9: **end if**
10: **end for**
11: Obtain the N_m-element possible index set $(\Lambda_1, ..., \Lambda_{N_m})$ using L_1, L_2, L_3, L_4.
12: Obtain the optimal index $\hat{q}$ by (31).
13: $\Lambda = \Lambda_{\hat{q}}$.
14: $\mathbf{s}$ can be obtained by (30) using Λ.

Step 5: Based on the results of Steps 3 and 4, the final results can be estimated as

$$\hat{q} = \underset{q \in (1, N_m)}{\arg\min} \left\| \hat{\mathbf{y}} - \tilde{\mathbf{W}}_{\Lambda_q} \mathbf{s}_q \right\|^2. \tag{31}$$

In summary, the detail process of the E-BCS detector is shown in Algorithm 1.

VI. Simulation Results

In this section, the performances of the proposed STBC-QSM systems are presented and compared in Figs. 1 and 4. In all the simulation results, perfect channel state information is assumed. Specifically, Fig. 1 compares the performance of the proposed STBC-QSM system to that of the DA-QSM system [14] and of the ESM-ATA system [13] having $N_t = 4$, $N_r = 4$ at 4 bits/s/Hz and $N_t = 8$, $N_r = 8$ at 6 bits/s/Hz. ML detectors are employed in these systems. Moreover, the theoretical performances of the proposed STBC-QSM system are also added. As seen from Fig. 1, the upper bound derived becomes very tight upon increasing the SNR values for the proposed STBC-QSM schemes, which is helpful for evaluating the BER performances. It is also shown that the STBC-QSM scheme advocated is capable of outperforming the DA-QSM system and the ESM-ATA scheme by 1.5 dB and 3.5 dB at BER=10^{-5}, respectively.

Fig. 2 compares the performance of the ML detector based STBC-QSM system to that of the QSM system having $N_t = 4$, $N_r = 2$ at 6 bits/s/Hz and $N_t = 8$, $N_r = 2$ at 8 bits/s/Hz. In this case, 16-QAM is employed in the STBC-QSM system, while QPSK is employed in the QSM system. Observe from Fig. 2 that the proposed STBC-QSM system is capable of outperforming the QSM system by 7.5 dB for both of the above setups.

Fig. 3 and Fig. 4 compares the performance of the proposed E-BCS detector to that of the detectors recently developed for the proposed STBC-QSM system having $N_t = 4$, $N_r = 4$ at 4 bits/s/Hz and $N_t = 8$, $N_r = 8$ at 6 bits/s/Hz, respectively. The parameters of $V_{\text{th}}^1 = 0.1$ and $V_{\text{th}}^2 = 10$ are employed by the proposed E-BCS detector, which are obtained from our simulation statistics. Observe from Fig. 3 that the performance of the proposed E-BCS detector associated with the above thresholds is capable of approaching the ML detector and outperforming the existing MMSE, ECS [15] and BCS [16], detectors. Similar trends can also be observed for the case of $N_t = 8$ and $N_r = 8$ in Fig. 4.

TABLE II
Average number of searching candidates of different detectors for the proposed STBC-QSM system.

$N_t = 4, N_r = 4, Rate = 4bits$					
	SNR=0 dB	4 dB	8 dB	10 dB	12 dB
ML	2^8	2^8	2^8	2^8	2^8
MMSE	1	1	1	1	1
BCS [16]	1	1	1	1	1
ECS [15]	3	6.0	7.6	7.7	7.7
Proposed $m = 2$	6.1	4.2	2.2	1.6	1.2
$N_t = 8, N_r = 8, Rate = 6bits$					
	SNR=0 dB	4 dB	8 dB	10 dB	12 dB
ML	2^{12}	2^{12}	2^{12}	2^{12}	2^{12}
MMSE	1	1	1	1	1
BCS [16]	1	1	1	1	1
ECS [15]	31	88	108.8	113	110
Proposed $m = 2$	11	6.4	2.6	1.6	1.1
Proposed $m = 3$	43	23	6.2	2.6	1.5

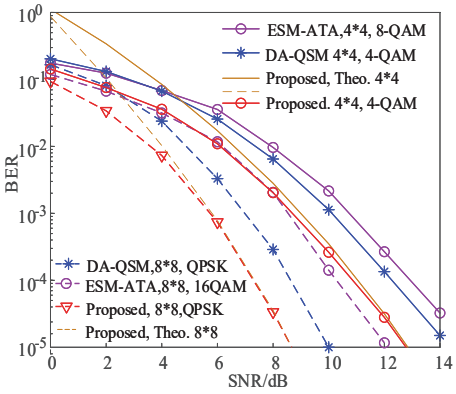

Fig. 1. Performance comparison between the proposed STBC-QSM scheme and the DA-QSM and ESM-ATA schemes at 4 bits/s/Hz and 6 bits/s/Hz.

As for their complexity comparison, the complexity of the above detectors is mainly dominated by the average number of search candidates, which are shown in Table II. Observe from Table II that the average number of search candidates for the proposed E-BCS detector is close to one in the high-SNR region. To elaborate in high SNR region, there may be only very few STBC-QSM symbols that are estimated inaccurately by the BCS detector, while the proposed thresholds based E-BCS detector is capable of handing these inaccurate symbols efficiently. By increasing the number of search paths, these inaccurate symbols are still likely to be finally accurately detected. As a result, the proposed E-BCS detector is capable of approaching the ML detector's performance at a complexity similar to that of the MMSE detector.

VII. Conclusions

In this paper, a novel STBC-QSM based MIMO system is proposed, which endows the QSM system with a diversity gain by incorporating the classic STBC structure.

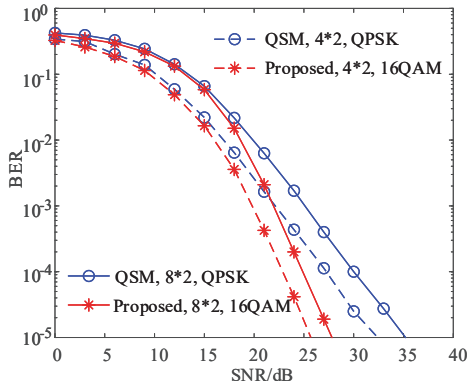

Fig. 2. Performance comparison between the proposed STBC-QSM and the QSM schemes at 6 bits/s/Hz and 8 bits/s/Hz.

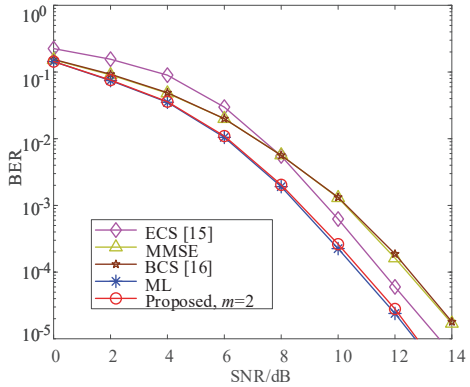

Fig. 3. Performance comparisons of the proposed E-BCS detector and of the existing detectors for the proposed STBC-QSM system having $N_t = 4$ and $N_r = 4$ at 4 bits/s/Hz.

Furthermore, an efficient Bayesian CS detector is proposed for our STBC-QSM system. Our simulation results have shown that the proposed STBC-QSM system is capable of providing considerable performance gains over both the recently developed DA-QSM and ESM-ATA systems for any setups having the same transmission rate, as well as providing more than 7.5 dB performance gain over the QSM system with one or two receiver antennas. Moreover, the E-BCS detector proposed for our STBC-QSM system is capable of approaching the ML detector's performance at the MMSE detector's complexity in the high-SNR region. The performance of the QSM system combined with generalized STBC and that of imperfect channel estimation will be considered in our future work.

References

[1] R. Mesleh, S. S. Ikki, and H. M. Aggoune, "Quadrature spatial modulation," *IEEE Trans. Veh. Technol.*, vol. 64, no. 6, pp. 2738-2742, June. 2015.

[2] R. Mesleh, H. Haas, S. Sinanovic, C. W. Ahn, and S. Yun, "Spatial modulation," *IEEE Trans. Veh. Technol.*, vol. 57, no. 4, pp. 2228-2241, Jul. 2008.

[3] J. Li, M. Wen, X. Cheng, Y. Yan, S. Song, and M. H. Lee, "Generalised pre-coding aided quadrature spatial modulation," *IEEE Trans. Veh. Tech.*, vol. 66, no. 2, Feb. 2017.

[4] A. Afana, I. A. Mahady and S. Ikki, "Quadrature spatial modulation in MIMO cognitive radio systems with imperfect channel estimation and limited feedback," *IEEE Trans. Commun.*, vol. 65, no. 3, March, 2017.

[5] A. Younis, N. Abuzgaia, R. Mesleh and H. Hass, "Quadrature spatial modulation for 5G outdoor millimeter-wave communications: Capacity analysis,"*IEEE Trans. Wireless Commun.*, vol. 16, no. 5, May, 2017.

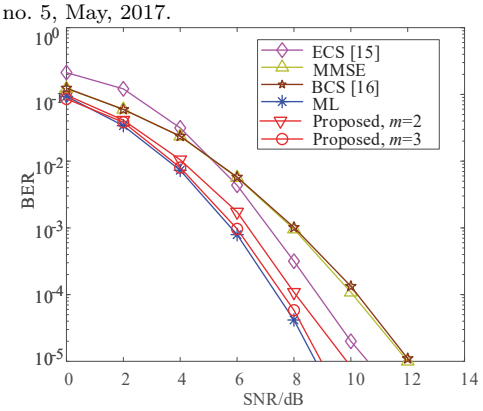

Fig. 4. Performance comparisons of the proposed E-BCS detector and of the existing detectors for the proposed STBC-QSM system having $N_t = 8$ and $N_r = 8$ at 6 bits/s/Hz.

[6] S. Althunibat and R. Mesleh, "Performance analysis of quadrature spatial modulation in two-way relaying cooperative networks," *IEEE IET*, vol. 12, no. 4, pp. 466-472, 2018.

[7] A. Younis, R. Mesleh and H. Haas, "Quadrature spatial modulation performance over nakagami-m fading channels," *IEEE Trans. Veh. Technol.*, vol. 57, no. 4, pp. 2228-2241, Jul. 2008.

[8] L. Xiao, P. Yang, S. Fan, S. Li, L. Song, and Y. Xiao, "Low-complexity signal detection for large-scale quadrature spatial modulation systems"*IEEE Comun. Lett.*, vol. PP, no. 99, pp. 1-4, Aug., 2016.

[9] R. Mesleh, S. Althunibat and A. Younis,"Differential quadrature spatial modulation,"*IEEE Trans. Commun.*, vol. 65, no. 9, Sep., 2017.

[10] B. Zheng, F. Chen, M. Wen, F. Ji, H. Yu, and Y. Liu, "Low-complexity ML detector and performance analysis for OFDM with inphase/Quadrature index modulation,"*IEEE Comun. Lett.*, vol. 19, no. 11, pp. 1893-1896, Aug., 2016.

[11] E. Basar, U. Aygolu, E. Panayirci and H. V. Poor, "Space-Time Block Coded Spatial Modulation," *IEEE Trans. Commun.*, vol. 59, no. 3, pp. 823-832, Mar. 2011.

[12] S. Althunibat, R. Mesleh, "Enhancing spatial modulation system performance through signal space diversity," *IEEE Commun. Lett.*, doi: 10.1109/LCOMM.2018.2817621.

[13] L. Xiao, Y. Xiao, L. You, P. Yang, S. Li and L. Hanzo, "Single-RF and Twin-RF spatial modulation for an arbitrary number of transmit antennas," *IEEE Trans. Veh. Tech.*, vol. pp, no. 12, Dec. 2017.

[14] L. Wang, Z. Chen, Z. Gong and M. Wu,"Diversity-achieving quadrature spatial modulation," *IEEE Trans. Veh. Tech.*, vol. 66, no. 12, pp. 10764-10775, Dec. 2017.

[15] L. Xiao, Y. Xiao, C. Xu, P. Yang, S. Li and L. Hanzo. Compressive sensing assisted spatial multiplexing aided spatial modulation. *IEEE Trans. Wireless Commun.*, vol. 17, no. 2, Dec. 2018.

[16] D. Wipf and B. D. Rao, "An empirical bayesian strategy for solving the simultaneous sparse approximation problem," *IEEE Trans. Signal Process.*, vol. 55, no. 7, pp. 3704-3716, July, 2007.